



4-1984

Characterization of a High Solids TiO_2 – Dispersant System at High Rates of Shear

Stephen R. Holmes
Western Michigan University

Follow this and additional works at: <https://scholarworks.wmich.edu/engineer-senior-theses>

 Part of the Wood Science and Pulp, Paper Technology Commons

Recommended Citation

Holmes, Stephen R., "Characterization of a High Solids TiO_2 – Dispersant System at High Rates of Shear" (1984). *Paper Engineering Senior Theses*. 208.
<https://scholarworks.wmich.edu/engineer-senior-theses/208>

This Dissertation/Thesis is brought to you for free and open access by the Chemical and Paper Engineering at ScholarWorks at WMU. It has been accepted for inclusion in Paper Engineering Senior Theses by an authorized administrator of ScholarWorks at WMU. For more information, please contact wmu-scholarworks@wmich.edu.



Characterization of a High Solids TiO_2 - Dispersant
System at High Rates of Shear

By
Stephen R. Holmes

A Thesis Submitted to the Faculty of the
Department of Paper Technology in Partial Fulfillment
of the Degree of Bachelor of Science

Western Michigan University
Kalamazoo, Michigan
April 21, 1984

ABSTRACT

The objective of this research was to study rheograms of high solids titanium dioxide dispersions at different dispersant levels. Viscometric measurements were collected with a Hercules High-Shear Viscometer. Viscosity was calculated using the initial slope of the increasing shear rate flow curve from the rheogram. This technique was incorporated to calculate viscosity in the laminar region up to the critical shear rate, where flow instability was expected to develop according to Taylor vortical flow calculations. The dispersant levels (dispex) were varied based on grams of titanium dioxide at varying percent solids levels. The results were evaluated according to a two-phase model for high solids dispersions at high shear rates. Based on this approach, the continuous (dispersing) phase is being sheared inside the effective gap determined by the volume occupied by the pigment solids. At the same solids volume concentration a parameter, defined as Relative Shear Volume (RS'V), was expected to indicate the packing array of solids under strong hydrodynamic conditions.

It was found that upon increasing dispersant levels that the gap percent reduction decreased and the relative shear volume increased. These results indicated that the pigment particles were packed more efficiently under shear as the dispersant level increased.

Keywords: Rheology, Dispersions, Solids Content, Titanium Dioxide, Viscosity

TABLE OF CONTENTS

	<u>Page</u>
ABSTRACT	
I. RHEOLOGY - ITS IMPORTANCE.....	1
II. OBJECTIVES OF STUDY.....	1
III. HISTORICAL DEVELOPMENT OF RHEOLOGY.....	2
IV. THEORY.....	5
A. Definitions of Terms Used.....	5
B. Science of Rheology.....	8
C. Types of Flow.....	11
1. Dilatant Flow.....	12
2. Newtonian Flow.....	12
D. Viscosity Measurement.....	13
E. Dispersion Parameters.....	15
1. Secondary Forces DLVO Theory.....	19
V. NEW THEORY OUTLINED.....	21
VI. EXPERIMENTAL DESIGN.....	23
A. Dispersant Addition.....	26
B. Titanium Dioxide.....	26
VII. RESULTS PRESENTATION.....	29
A. Effective Gap (X_{EFF}).....	29
B. Percent Reduction (% Red).....	30
C. Relative Shear Volume (RS^1V).....	31
D. Taylor's Model.....	31
E. Percent Solids.....	32
VIII. CONCLUSIONS.....	33
IX. FOR FURTHER STUDY.....	34

Table of Contents - Cont'd

	<u>Page</u>
Tables	
Table 1.....	23
Table 2.....	24
Figures	
Figure 1.....	9
Figure 2.....	11
Figure 4.....	14
Figure 5.....	41
Figure 6.....	42
Figure 7.....	43
Figure 8.....	44
Figure 9.....	45
Figure 10.....	46
Figure 11.....	47
References.....	35

I. RHEOLOGY - ITS IMPORTANCE

The importance of the study of Rheology of pigment suspended systems has grown greatly in the past few years. With new technology being applied in the paper industry, a thorough knowledge of flow properties and conditions affecting these properties is essential for productive and quality product manufacture, for example; the use of higher coating solids with increased machine speeds contributing to higher shear rates.

II. OBJECTIVES OF STUDY

The purpose of this study was to determine the effects of varying dispersant levels on a high solids TiO_2 -water system at high shear rates applying new rheological theories.

The Hercules Hi-Shear viscometer was used to apply high shear rates to the above outlined system. The rheograms produced were analyzed, in conjunction with a specified solids and dispersant level, and the data formulated was then applied to new theories.

III. HISTORICAL DEVELOPMENT OF RHEOLOGY

Magnified interest in the field of Rheology did not actually occur until the twentieth century. Before then, its development and application was a slow process. The first peoples to actually apply Rheology were the Sumerians. They demonstrated that a specific weight measurement could be obtained by monitoring the flow-rate of water flowing from a funnel per unit time. By the year 1540 B.C., a 1500 year time span after the Sumerians, Amenemhet, an Egyptian, became the first rheologist documenting and developing flow properties of fluids. From his experimentation, he invented a process to measure time through the observation of the water level, in a cone-shaped instrument, as water flowed from the bottom. His studies involved the flow behavior of different liquids, and even made corrections for fluid viscosity and flow-rate changes with variations in temperature.

Development then stagnated and not much advancement occurred until the Renaissance period, in the 16th century, when Leonardo DaVinci investigated water flowing through orifices and channels(2). DaVinci's studies and observations built a strong foundation on which later studies were based.

Galileo and Robert Hooke, in the 17th century, were instrumental in experimentally showing that stress is proportional to strain in elastic solids(2). Also, Sir Isaac Newton made major contributions by studying the flow in liquids, and observed that the resistance of a liquid to flow is proportional to the rate of shear². Newton made lasting contributions and actually was the first to develop a rotational viscometer, which consisted of a rotating cylinder submerged in a pool of water, where the speed of rotation could be controlled providing variable shear rates. This basic design is still in use today, in many rotational viscometers, including the Hercules Hi-shear Viscometer which will be discussed, in detail, later in this report.

Newton's work and derived laws were associated with the Rheology of water; thus, fluids which behave like water are termed Newtonian fluids, and their flow can be described accurately applying Newton's laws. Today, rheologists use these laws only as an idealized case and many modifications have been and are still occurring to describe the flow of materials in which the shearing stress is not linearly proportional to the rate of shear.

Poiseuille, in the mid-19th century, studied the flow of human blood in the veins and capillaries of the body; then extended his work to include the flow of water through glass capillary tubes as a dynamic model for blood flow. From his experimentation, he discovered that the liquid flow-rate through the tube was dependent on the diameter of the tube, the applied pressure, along with the viscosity of the liquid and tube length. This relationship called Poiseuille's Law is expressed as:

POISEUILLE'S LAW

$$V = \frac{\pi (d/2)^2 (P_1 - P_2)}{8 \eta L}$$

Where V = Flow delivered per second (cm³/sec.)

d = diameter (cm)

η = Viscosity in Poises (g/cm-sec)

L = length (cm)

P = pressure (g/sec²-cm)

In honor of Poiseuille, the unit describing viscosity is the term "Poise."

From the beginnings of the study of Rheology, outlined to the present century, an explosion of research and development has been reported, and a newly published theory used in this research will be outlined in the following section(1).

IV. THEORY

A. Definitions of Terms Used¹:

1. Apparent Viscosity - The ratio of shear rate to shearing stress for non-Newtonian fluids indicating viscosity variations with shear.
2. Break Point - The point at which a change in slope on a Rheogram is seen and corresponds to the onset of unstable flow.
3. Coefficient of Viscosity - N is a proportionality factor applied to Newtonian liquids which states that shear rate (dv/dx) is proportional to shear stress (F/A).

$$N = (F/A)/(dv/dx)$$

4. Critical RPM - CTRPM - the rpm at the break point

5. Poise - Unit defining viscosity of fluids

Poise = dyne-sec/cm² or g/cm· sec

6. Shear Rate - The velocity gradient or difference between successive adjacent lamina of a fluid during flow.
7. Shear Stress - Force per unit area (dyne/cm²) applied to a fluid which causes flow.
8. Viscosity - Intrinsic property of a material resisting applied stresses which impact flow.
9. Effective clearance (χ_{EFF}) - calculated using the coefficient of viscosity (N) and the continuous phase viscosity (N_0) which takes into consideration the area being occupied by particles in the continuous phase.

$$N = \frac{F/A}{dx/vx} \quad , \quad N_0 = \frac{F/A}{dv/dx_{EFF}}$$

$$N_0/N = dx_{EFF}/dx_0$$

$$\chi_0 = \text{gap dimension}$$

NOTE: Shearing Force (F/A) is equal for N and N_0

Velocity difference is also equal for N and N_0

$$\text{Thus, } X_{\text{EFF}} = \frac{N_0 dx_0}{N}$$

and is a function of the percent solids and original gap x_0 .

$$10. \text{ Gap Reduction - \% Red} = \frac{X_0 - X_{\text{EFF}}}{X_0}$$

is an indicating factor of how a system's particulates are packing and effecting gap dimensions.

$$11. \text{ Relative Shear Volume - RS/V} = \frac{\% \text{ Red}}{\% \text{ Solids}}$$

This computation is the occupied pigment volume divided by the theoretical pigment volume.

12. Taylor's Formula¹ - Devised by Taylor in 1923, calculating the critical angular velocity for the onset of unstable flow is expressed:

$$W_{\text{cr}}^2 = \frac{\pi^4 n^2 (R_1 + R_2)^2}{2 d R_1^2 P X_0^3}$$

$$\text{RPM}_{\text{cr}} = \sqrt{W_{\text{cr}}} \times 30/\pi$$

Where N = App. Viscosity

R_1 = radius of Bob

R_2 = radius of cup

χ_o^3 = calculated gap

d = density

P = approximately χ_o/R_1 in this Research for Bob

$$A = 0.0571$$

13. Critical Rpm - $RPM_{cr} = \sqrt{W_{cr}} \times 30/\pi$

(21 (rpm) = W) RPM at which unstable flow occurs

B. Science of Rheology

Rheology is the science of deformation and flow of matter. It is considered a branch of the Natural Sciences, an area between chemistry and physics, concerned with the flow characteristics of matter.

Viscosity is a physical property (defined previously) of matter which is a standard for the internal friction of a substance. As a result, a substance's internal friction resists flow and forces or

stresses are required in order to create flow in such a material². Since all substances; gas, liquid, and solid exhibit internal friction, higher or lower viscosities can be assigned to each. The principle of the viscosity of a substance is illustrated by the following, well-known parallel plate experiment (Figure 1).

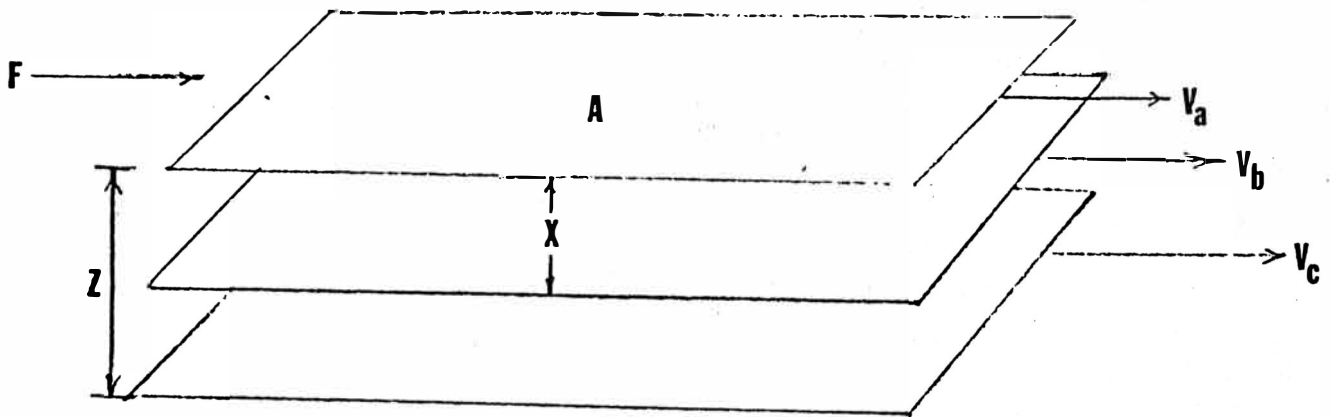


FIGURE 1

Two plates of the same size having an area A [cm^2] are arranged parallel with respect to each other. A substance is located between the plates separating them a certain distance X [cm]. A force F [dyne] is then applied to one of the plates, and the plate is displaced. Thus, a shear stress τ acts on the plate and in the substance.

$$\tau = \frac{F}{A} [\text{dyne} \cdot \text{cm}^{-2}]$$

As a result of this shear stress, the plate accelerates and then assumes a constant velocity V [$\text{cm} \cdot \text{sec}^{-1}$]. A velocity or shear gradient D is thus formed in the substance because the substance adheres to both the moving and fixed plates.

In this experiment, the lamella or individual layers of the substance are displaced, with respect to each other, and a regular gradation of velocity is passed from one lamella to the next (laminar flow). In this manner, the internal friction of the substance must be overcome through the shear stress³. The shear gradient D is expressed:

$$D = \frac{dv}{dx} [\text{sec}^{-1}]$$

Where dx is perpendicular to the direction of flow.

The shear gradient is the velocity difference between two neighboring layers of the substance divided by their distance.

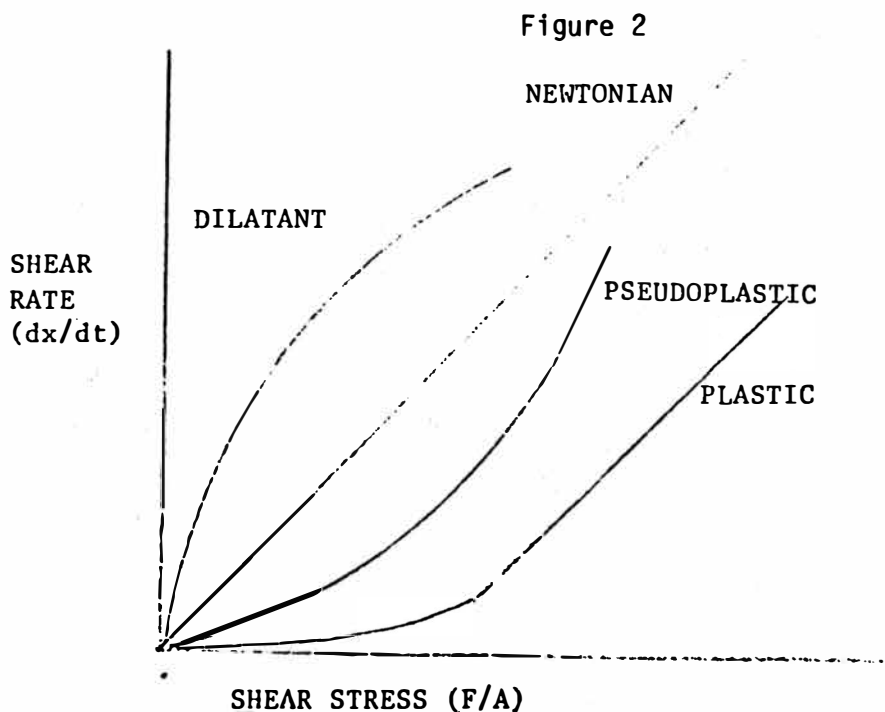
Applying the shear stress τ , the shear gradient D , and the viscosity η to Newton's law: $\tau = \eta D$

The relationship between shear stress and shear rate can then be expressed as:

$$\frac{F}{A} = \eta \frac{dv}{dx}$$

C. Types of Flow

In the study of Rheology, there are four basic types of flow which can be represented by a plot of shear rate dx/dt versus shear stress F/A , and are shown in the following figure:



Of main importance in this research is Newtonian flow and briefly understanding dilatant flow. Therefore, Newtonian and dilatant flow behavior is defined.

1. Newtonian Flow

The characteristic of Newtonian flow is that the rate of shear is proportional to the shear stress and the viscosity remains constant, independent of the shear rate.

Thus, for a Newtonian material, a plot of shear rate versus shear stress yields a linear line with a Y-intercept of zero and the slope equal to viscosity, which is shown graphically in Figure 2.

2. Dilatant Flow

As an increasing shear rate is applied to a substance with no measurable time dependence, an isothermal reversible increase in viscosity occurs; this behavior is termed dilatancy. When particle suspensions which are fluid at rest are subjected to shear, the viscosity increases, in some cases, to such a degree that the suspension behaves almost as a solid. This occurrence is descriptively called "shear rate thickening", and the flow curve is concave to the shear stress axis and is shown in Figure 2 compared with flow curves of other types of flow.

When a suspension is at rest, the particles are able to fit into the voids of adjacent layers, but under high shear conditions, layers of particles begin gliding over adjacent layers. Thus, a volume expansion occurs (volumetric dilatancy) under high shear rates because of the particles inability to fill the voids which causes the viscosity to increase, and this phenomenon has been given the term "shear blocking."

D. Viscosity Measurement

In this research, a Hercules Hi-Shear viscometer was used to make viscosity measurements. The Hercules is a rotational cup and bob viscometer where the inner cylinder is rotated and the stress is measured at the outer cylinder surface. The inner cylinder or bob is immersed in the sample and driven by a variable speed motor. As a result of the rotating bob, a viscous drag is imparted on the outer cup causing a rotational deflection which is sensed by two springs attached to the cup through a wrapped string arrangement with an affixed pen. The deflection is, therefore, traced by the pen on graph paper which provides a continuous curve of shear rate (RPM, Y-axis) versus shear stress (torque (dyne·cm), X-axis).

Figure 4 depicts the Hercules cup and bob configuration.

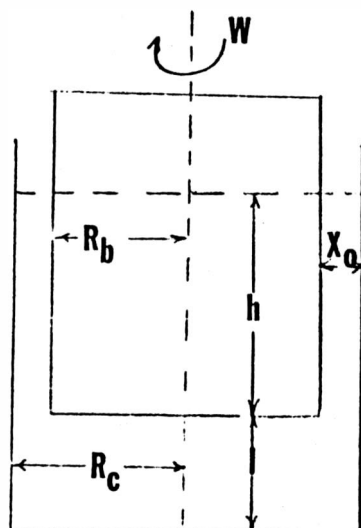


Figure 4

Where:

R_b = radius of bob

R_c = radius of cup

W = speed of rotation

h = effective depth of sample

l = distance from the bob to
cup

Hercules Hi-shear calculations are expressed:

Apparent Viscosity

$$\eta = \frac{9.55 \times T \times S}{\text{RPM}} \text{ in poises}$$

Where:

T = torque (spring constant \times deflection in cm X-axis)

S = bob constant (0.0002)

NOTE: In this research, bob A was used exclusively

RPM = cm upon Y-axis

9.55 = Instrument Constant

See Appendix I for Hercules Hi-shear operating instructions.

E. Dispersion Parameters

Dispersion is of main importance when dealing with pigment particles and depends on the chemical treatment to promote deflocculation (or decoagulation) and mechanical treatment to promote disaggregation. Chemical treatment is usually the addition of a dispersing agent, which is added to overcome the coagulation (clump formation and attraction between particles), properties of the pigment particles. In order for disaggregation, the chemical dispersant must be present to insure that the mechanical power is applied upon the aggregate and not dissipated against flocculation. Therefore, a chemical agent needs to be added initially before the mechanical power.

It has been reported that the interparticle attraction is due to an imbalance of the chemical forces at the surface of the particles owing to the aggregating and flocculating of particulate material⁸. Thus, the dispersing agent has to eliminate particle

attractions and prevent the particles from coming into intimate contact with one another and flocculating. DeWaeles states that deflocculation depends on the formation of a barrier on the dispersed particles surface which is thicker than the distance at which their surface attractive forces are significant⁴.

Dispersion, therefore, begins after the dispersant ionizes and is absorbed onto the pigment surface. The charge of the absorbed ion is then localized at the particles surface giving that particle an electrostatic charge equal to the ion. The magnitude of the charge depends on the charge and number of ions adsorbed. There is no change in the net balance of positive and negative charges in the system, but the charges are distributed. The ions adsorbed are removed from the solution leaving the other positively or negatively charged ions in solution. The pigment particles, thus, have an extra concentration of ions of one charge on their surface and the solution surrounding the particle contains an extra concentration of ions of the opposite charge. An ionic electric double layer is then formed, because of the attraction of the particles with the oppositely charged ions of the solution. This is the basic concept and theory behind the stability of lyophobic colloids.

The ions that are in excess in solution, as a result of the adsorption of the oppositely charged ions on the pigment surface, are called counter-ions. The factors which caused the dispersant to ionize makes the separation of (+ and -) ions stable and the counter-ions do not attach themselves to the oppositely charged ions on the particle surface. These counter-ions make the particles repulsive to one another and forms a stable dispersion. The ability of a substance to form a double-layer, as described, is the property of a dispersant.

The counter-ions have some important properties:

1. They are distributed in a layer around the pigment and held in place through the attraction of the adsorbed ions.
2. The counter-ion layer is quite thick, approximately 10\AA , while the adsorbed ions on the pigment surface are concentrated and only one ion thick, approximately 1\AA .
3. The counter-ions do not cluster tightly around the adsorbed ions nor cluster around themselves. They are distributed with the highest concentration next to the pigment surface and their concentration decreases as the distance from the particles surface increases.

Pigment particles, therefore, repel one another because of the similarly charged counter-ion layers surrounding each particle, and flocculation does not occur.

Particles, as mentioned previously, do have attraction for one another when they are very close together. These forces of attraction between molecules are secondary forces which will be explained later. The forces of repulsion from the counter-ion layer are significant at long distances (100\AA); whereas, attraction forces between particles only occur at small distances, on the order of $10\text{-}30\text{\AA}$, so dispersion is made possible.

Dissolved electrolytes in solution tend to collapse the counter-ion layer moving it closer to the particle surface.. A thin cloud allows the particles to approach one another closely increasing the probability of secondary attractive forces taking over and causing flocculation.

If surface attractive forces are prevented, the viscosity or flow of the system will be associated with the volume that the pigment particles occupy and their collisions. Dispersion is then related to viscosity and a dispersant is described, through its

ability to minimize the viscosity of a system at a certain concentration, while adequate mechanical forces are supplied to the suspension.

1. Secondary Forces - DLVO Theory

When the continuous phase is water, ionization of a dispersant occurs and free ions are adsorbed with the particles possessing an electrical double-layer explained above. When the counter-ion layers of similar particles overlap, a net repulsive force results. These double-layer forces can be combined with the attractive forces, due to London VanderWaal's forces to give a net interaction. VanderWaal's forces are secondary bonding forces created when electrically neutral molecules have dipole moments or a displacement of their charge. These forces are weak and easily broken, and are responsible for viscous deformation. Both of these interactions are dependent on the degree of particle separation, and the result is that the net interaction also depends on the interparticle separation⁴.

Work published by Verwey, Overbeek, Derjaguin, and Landau has shown that the addition of an electrolyte reduces the energy barrier and prevents aggregation until a point is reached where no barrier remains⁵. When this energy barrier is surpassed, aggregation becomes more rapid owing to net attractive forces at other values of the particle separation⁵. Also, the effect of the size of particles on the interaction energy was noted that when particles are smaller than the double-layer, stability always increases with increased particle size, because the counter-ion repulsion is more significant than the dispersion forces. Conversely, as the concentrations of electrolyte approaches a critical flocculation concentration, the range of the electrical double-layer and dispersion forces are reversed⁵. Dispersion forces are developed as the electrons move around the nuclei of the molecule and dipoles, which are continuously changing, have a mutual attraction and effect the molecules nearby.

V. NEW THEORY OUTLINES

The data that has been obtained through this research has been applied to a newly formulated theory which has recently been published¹. This theory states that in a pigment dispersion, the particles just take up space leaving the continuous phase, in this case water; the phase being sheared. Thus, a layer of continuous phase is subjected to a shear rate while the dispersed particle phase is in a plug flow configuration¹. Thus, it is understood that the two different phases, the liquid being the continuous and the solid or pigment the dispersed phase, act separately when shear is induced. With the solid particles occupying space, the continuous phase is subjected to a shear rate.

The continuous phase is being sheared in the center of, the gap between the cup and bob of the viscometer, while the dispersed phase is positioned along the shear inducing boundaries or near the cup and bob walls.

Logically, the number and size of particles present in the suspension affect the available space for shear. As the percent of solids increases, the available space for shear decreases, requiring higher velocities and shear rates to reach flow instability. Therefore, when

the viscosity of a material is being calculated, using a Hercules Hi--Shear Viscometer, the gap between the bob and cup is erroneous unless the volume that the dispersed phase is displacing is considered and a new, corrected clearance is calculated. This new clearance is reported as the effective clearance χ_{EFF} and the volume occupied by the dispersed phase is calculated (see "Definitions of Terms Used").

Without using the χ_{EFF} clearance, erroneous viscosities will be calculated because of the shear rates dependence on the gap dimensions.- The χ_{EFF} (effective clearance) is calculated using N_0 , the true viscosity of the continuous phase, a derivation of χ_{EFF} is shown previously in this report, and is a function of the percent solids and the original gap χ_0 (cm)¹.

The rheograms generated were evaluated at the breakpoint following the first Newtonian region. This rheogram, shown in Figure 5, details a linear Newtonian portion with a break point followed by a second Newtonian region which separates itself from a dilatant rheogram (see Figure 2). The break point, outlined above, and change of slope can be associated with unstable flow. A model proposed by G.I. Taylor, in 1923, mathematically predicts the critical angular velocity for unstable coaxial couette flow as is found in a rotational viscometer; such as,

the Hercules. In this manner, the nature of the experimentally observed break point can be defined and analyzed.

Also, two other calculations are used; the Percent Gap Reduction (% Red) and the Relative Shear Volume (RS^1V) with Taylor's model to establish the effects, percent solids, and dispersant level have on the gap dimensions¹.

VI. Experimental Design

This study was to investigate a high-solids TiO_2 -water system under high-shear and varying dispersant levels. The parameters varied were percent solids, dispersant level, and spring load (see Table I).

Table I

%Solids		45	Dispersant Levels for Each % Solids 1,2, 4, 6, 8 mg/g based on g TiO_2	
		50		
		55		
			Spring sets were varied for each solids level at each dispersant level - 25,000, 50,000, 100,000 (dyne cm/cm)	
Dispersant Level mg/g	% Solids	45	50	55
	1	25,000 spring sets		
	2	50,000		
	4	100,000		
	6			
	8			

Rheograms were then run using the Hercules on each solids level; 45, 50, 55 at each dispersant level; 1, 2, 4, 6, 8 mg/g; and using three spring sets: 25,000, 50,000, 100,000 dyne cm/cm.

Certain experimental design precautions were taken to reduce variability and ensure concluding results. These are shown in Table II. The exact experimental procedure is outlined in Appendix II of this report. The percent solids and dispersant levels used were determined through preliminary experimental trials.

Table II

EXPERIMENTAL DESIGN PRECAUTIONS

1. Procedure will be timed and controlled from preparing the TiO_2 slip through mechanical energy imparted to system and testing of dispersed slip.
2. The temperature, water hardness, and pH will be controlled to minimize variability in dispersion and viscosity.
3. The shear applied to each % solids dispersion will be controlled.
4. A Brookfield at 20 RPM will be run before each Hercules test in order to collaborate data.
5. The same bob, and RPM* will be held constant to minimize errors and differences.
6. A systematic system was established to evaluate rheograms and minimize error.

* Except where higher shear rates (> 4400 RPM) are needed.

In this study, the slips were dispersed using a Cowles Dissolver at 2,650 rpm (*See Appendix II - "Experimental Procedure") for 45 minutes. The Cowles Dissolver depends on kinetic energy and dispersing action is developed between the agitator and the pigment.

The vicinity surrounding the high RPM rotor is a turbulent high energy area where energy is imparted to the pigment fluid and dispersion takes place. For a well-dispersed system, all the particles must pass through the area of highest shear and is time-dependent. Optimum dispersion will be attained for each mixing intensity after which additional agitation under identical conditions gains little. To improve dispersion and reduce mixing time, higher agitator speeds raise the energy imparted to the aggregates and the material passes through the area of highest intensity more often. Also, dispersion is improved as the pigment concentration increases because of increased shearing forces being produced by the higher viscosity and an increased particle-particle interference⁶.

It has been reported that an increase in mixing intensity reduces the resistance of the system to flow by reducing particle interference, and causing the system to engage less liquid when subjected to shear⁷.

A. Dispersant Addition

Mechanical and chemical factors must be taken into consideration when dealing with the sequence to be followed for particular coating formulation. In order for disaggregation the chemical dispersant must be present to insure that the mechanical energy is being applied upon the aggregate.

In a flocculated system, the mechanical energy is used inefficiently because particles deflocculated mechanically readily flocculate once the mechanical energy is reduced. Therefore, the chemical agent, Dispex, was added before the mechanical energy assuring an efficient disaggregation (see Dispersion Section).

B. Titanium Dioxide

Titanium is manufactured by two processes: 1) chloride, and 2) sulfate. Three forms of titanium dioxide are available: rutile, anatase, and brookite. Rutile is the most stable and important of the three forms mentioned and will be used in this research. Rutile is mainly made using the chloride process

which reacts titanium ore with gaseous chlorine and carbonaceous material at high temperature. Titanium tetrachloride, is separated and purified, and vaporized in oxygen to form the titanium dioxide crystals and chlorine. The pigment is then slurried or dried.

Titanium dioxide (mol. wt. 79.9), Rutile is derived from the Latin word meaning "red" through its association with reddish bauxite. Titanium dioxide pigment grades contain 60% Ti and includes Fe, Sn, Nb, and Ta. It has a tetragonal crystal structure and is chemically unreactive with materials used in coating systems.

In all three forms, each oxygen atom is bonded to three Titanium octahedra. The structure of Rutile differs from the other two in that each octahedron shares two oxygens with adjoining octahedra. In anatase, four oxygens are shared and in brookite three are shared⁵. The rutile structure is, therefore, more dense and compact with a higher specific gravity than anatase. Rutile also has a higher refractive index. Titanium dioxide has a much higher specific gravity

than clay or calcium carbonate and, therefore, behaves differently in high solids dispersions. Titanium dioxide also has strong agglomerative forces, and requires high-speed and energy mechanisms to produce a well-dispersed system.

VII. RESULTS PRESENTATION

The effects of varying dispersant levels on X_{EFF} , % Red, $RS^{1/V}$ will be analyzed in this section, along with comparisons of Taylor's model critical RPM, and the experimentally derived RPM calculated at the break point. Also, the effects of solids will be detailed.

A. Effective Gap (X_{EFF})

As outlined previously, the role of the particles is to take up space, thus, reducing the gap where the continuous phase can be sheared. Since the continuous phase is being sheared in a reduced gap, the actual shear rate is higher than that calculated assuming the full gap. the effective gap is then defined as the space available for the continuous phase to be sheared in the presence of the particle phase.

$$*\chi_{EFF} = \frac{N_0 dx_0}{N}$$

*Defined in Theory Section

As the dispersant level increases, the particle packing changes because of less aggregates, agglomerates, and floculate in the system. This can be concluded from Figure 7 which clearly shows decreasing viscosities with increased dispersant levels.

Higher χ_{EFF} values dictates a larger area for shear and flow enabling unstable flow to occur at decreased velocities, and this behavior is shown graphically in Figures 7 and 8. Through analysis of the break points in Figure 8 as the dispersant is increased, the break points become lower (lower RPM) which correlates with the conclusion drawn above.

B. Percent Reduction (% Red)

The percent reduction (% Red), of the gap is expressed as:
Percent Reduction = $(\chi_0 - \chi_e) / \chi_0$, and numerically indicates the decrease of the nominal gap at differing solids levels. Figure 9

details a trend that as the dispersant level is increased, the percent reduction decreases; thus, a conclusion can be drawn that the particles are packing more tightly occupying less space. This collaborates the conclusions drawn on the effects of dispersant level on X_{EFF} .

C. Relative Shear Volume (RS'V)

The Relative Shear Volume (RS'V) is a measure of the volume occupied by the pigment particles, thus, indicating the degree of particle flocculation.

$$RS'V = (\% \text{ Reduction} / \% \text{ Solids})$$

Figure 1D indicates that with increased dispersant the RS'V, which is in agreement with the statements and conclusions drawn pertaining to the effective gap and percent reduction, the system is more deflocculated and taking up less volume. This allows a larger area for shearing of the continuous phase.

D. Taylor Model

The Taylor formula, for the critical angular velocity for the onset of unstable flow, was calculated and compared to those measured experimentally from the break points on the rheograms. Taylor's

model did correlate with the experimentally calculated results, but was not totally conclusive. Some variation was seen (see Appendix III, "Data Table") ranging from ± 20 to ± 450 RPM from a maximum of 5,775 RPM. Taylor's model does apply and correlate with the break points enabling one to estimate the critical RPM at the onset of unstable flow, and enables one to draw a conclusion that the break point does associate with the onset of unstable flow.

E. Percent Solids

As the percent solids are increased, it is obvious that more particles are available to occupy more space decreasing the gap for the continuous phase to be sheared.

Figure 11 indicates that with increased solids, the velocity at the break point (RPM) does increase and collaborataes well with the explanations given of decreased effective gap. As the effective gap is decreased, the area for shearing of the continuous phase decreases and higher velocities are seen before the onset of unstable flow. Again, as in Figure 8 and 10, with increased dispersant levels lower velocities at the onset of unstable flow (lower break points) are noted.

VIII. CONCLUSIONS

In summary, increasing the dispersant level increases the effective gap (χ_{EFF}); whereby lower break points and velocities for unstable flow are reported because of a larger area (gap) for the shearing of the continuous phase.

The viscosities also were reported to decrease along with decreasing percent reduction (%Red) with increased dispersant levels. These occur because of a better dispersed, more efficient packing system with the particles occupying less space.

The relative shear volume (RS'V) increased with increasing dispersant levels indicating that the particles were occupying less volume and where less flocculated better dispersed packing more effectively.

Evaluating Taylor's formula for the critical angular velocity for the onset of unstable flow, compared to the experimentally calculated velocities at the break point in the rheograms, did correlate and could be used to estimate the critical RPM at the onset of unstable flow. As the percent solids were varied, the effective gap decreased and higher velocities (higher break points) were also noted.

In conclusion, the results of this research do collaborate and explain the theory outlined, stating that the continuous phase is the only phase being sheared and that the dispersed particle phase just occupies space is a viable theory.

IX. FOR FURTHER STUDY

This "new theory" has been experimentally shown to be viable, explaining the behavior of pigment dispersions. A topic for further study would involve: a more detailed study of the effects of solids, or moving on to yet a more practical and complicated system and its correlation to this proposed theory; determining ways in which to apply it practically in the paper industry.

References

1. Kline, J.E., "Rheology of High Solids Dispersions," TAPPI, 1983 Coating Conference, pp. 55-63.
2. Murray and Brodhag, "Paper Coating Pigments," Monograph No. 38, Atlanta, TAPPI, 1976.
3. Bogue, D.C. and Doughty, J.O., "Viscometric Measurements," Notes prepared for course in Polymer Rheology at the University of Tennessee, Knoxville, Tennessee, August 22-26, 1966.
4. Landes, C.G. and Kroll, Leonard, "Paper Coating Additives," TAPPI Press, Atlanta, 1978, pp. 15-32.
5. Garey, C.L. "Physical Chemistry of Pigments in Paper Coating," TAPPI Press, 1977, Atlanta, GA.
6. Willets, W.R., "The Rheology of Paper Coatings," TAPPI, Vol. 33, No. 4, pp. 201-208, April 1950.
7. Teirfolk, Jan-Erik, "The Flow Picture in the Mixer During Dispersing of Coating Pigments," Conference, Coating for the 1980's, TBPBIFL, Nov. 1980.
8. Parfitt, G.D., "Pigment Dispersion - In Principle and Practice," Tioxide Int. Ltd., Billingham, Cleveland, 1977, pp. 330-341.
9. Arnold, K.A., "Flow Properties of Coating Clays at High Rates of Shear," Paper Trade Journal, Vol. 117, No. 9, pp. 28-34 (August 26, 1943).
10. Baumeister, M. and Kraft, K., "Quality Optimization by Control of Coating Structure," TAPPI, Vol. 64, No. 1, pp. 85-89, January 1981.
11. Conard, P., "Rheological Properties of Coating Colors at High Shear Rates and Their Behavior on Blade Coaters," TAPPI, Vol. 57, No. 11, pp. 95-100, November 1974.
12. DeVries, T.C., "Fundamentals of Mixing," TAPPI, 1982 Blade Coating Seminar Notes, pp. 51-58 (1982).
13. Eklund, Dan, "High-Solids Coating Colors," TAPPI, Vol. 62, No. 5, pp. 43-48, May 1979.

References - Cont'd

14. Hagemeyer, R.W., "The Effect of Pigment Combination and Solids Concentration on Particle Packing and Coated Paper Characteristics," TAPPI, Vol. 43, No. 3, pp. 277-288, March 1960.
15. Hagemeyer, R.W., "The Influence of Chemical Composition on the Packing of Pigment Particles," TAPPI, Vol. 47, No. 10, pp. 575-598, October 1964.
16. Han, C.D., "Rheology in Polymer Processing," Chapter 9, Academic Press, New York (1976).
17. Heiser, E.J., "Latex, Blade Runability, Higher Solids Colors."
18. Kahila, S.J., Eklund, D.E., 1978 TAPPI Coating Conference, May 1-3, Denver, Colorado.
19. Klem, R.E. and Brogly, D.A., "Methods for Selecting the Optimum Starch Binder Preparation System," Pulp and Paper, May 1981.
20. Kline, J.E., "An Investigation of Adhesive-Pigment Interactions in Coating Mixtures," TAPPI, Vol. 55, No. 4, pp. 556-561, April 1972.
21. Lepoutra, P., "Paper Coatings: Structure-Property Relationships," TAPPI, Vol. 59, No. 12, pp. 70-75, Dec. 1976.
22. Lepoutra, P., "Paper Coatings: Substrate Absorbency and Coating Structure," TAPPI, 1978, pp. 61-68.
23. Mattson, V.F. and Leighton, J.R., "Progress Report on an Investigation of the Fundamental Factors Determining Coating Color Viscosities," TAPPI, Vol. 42, No. 1, January 1959.
24. Millman, Nathan, "Some Factors That Influence the Viscosity of Paper Coating Compositions," TAPPI, Vol. 47, No. 11, pp. 168a-174 (Nov. 1964).
25. Oittinen, Pirkko, "The Interactions Between Coating Pigments and Soluble Binders in Dispersions," TAPPI Coating Conf. 1981, pp. 113-122.
26. Patton, T.C., "Pigment Handbook Volume III Characterization and Physical Relationships," John Wiley & Sons, New York, 1973, pp. 43-130.

References - Cont'd

27. Price, C.R. and Hagemeyer, R.W., "Ultrafine Ground Calcium Carbonate - Its Use in Paper Coatings," TAPPI, Vol. 61, No. 5, pp. 47-50, May 1978.
28. Sennett, P., Massey, H.L., Morris, H.H., "Effect of Kaolin Pigment Particle Size and Shape on Rotogravure Print Quality," TAPPI, Vol. 65, No. 5, pp. 95-99, May 1982.
29. Triantafillopoulos, Nick, "The Effect of Alum and Polyacrilamides on inks," Term Paper Project, WMU 1982.
30. Upton, C. and Perkins, "Coating Raw Materials - Coated Paper Seminar Series II," St. Regis Technical Center, New York.
31. Walbaum, H.H., "Pigment Dispersion Property Evaluation by Scanning Electron Microscopy," TAPPI, Vol. 55, No. 7, pp. 1108-1114, July 1972.

APPENDIX I

PROCEDURE FOR OPERATING HERCULES HI-SHEAR VISCOMETER

The Hercules Hi-Shear Viscometer is a precision instrument that must be handled accordingly. In order to obtain reproducible rheograms, the following procedures were outlined:

1. Position coordinate paper on recording drum and carefully check the horizontal and verticle alignment.
2. Adjust recording pen to rest lightly at the origin.
3. Add proper amount of test specimens to the cup and position cup in the cup holder, making certain the cup is locked in position. The amount of test specimens added to the cup should be sufficient to just break over the top edge of the spindle when lowered to the operating position. (CAUTION: Do not over-fill the cup.) The level of test specimen is dependent upon the bob to be used.
4. Slowly lower spindle as far as it will go. Carefully close the top edge of the cup to prevent coating material from entering the spindle housing.
5. Remove cover on recording pen.
6. Reset and start test with RPM set at 4400.
7. When a spindle speed of 4400 RPM is attained as indicated by the LED, the AUTO mode will immediately decrease speed to zero at a uniform rate.
8. Lift pen from recording drum and replace cover. This will help insure clean rheograms free of blotting, etc.
9. Loosen spindle and remove cup and spindle for cleaning.

Special Precautions

1. Do not change position of the recording drum unless the locking nuts are loosened.
2. The cup holder is mounted on precision bearings that must be kept completely free of dust and foreign particles. Do not remove dirt particles from the base of the cup holder by blowing, but rather through the use of a fine brush, always brushing away from the bearing mounts.

Appendix I - Cont'd

3. The spindle housing and bearings therein is the most precise point of the instrument. Extreme care must be exercised to prevent coating from entering this assembly. Binding of the spindle in the housing will develop if this occurs.
4. The spindle and cup must be handled with care to prevent marking and burring. Do not place spindles on a hard, abrasive surface.
5. The spring sets should be kept dry and clean as they are carefully calibrated.
6. Temperature of the test specimens is important and will affect the viscosity determinations markedly. Results will be comparative at any one temperature level.

APPENDIX II

Experimental Procedure

A. Dispersion

1. Cowles Dissolver @ 2,650 RPM; Impellar 2 inches; Steel Beaker 6x9 inches
2. 1000 g Dry Basis Pigment; Distilled H₂O and Dispex Dispersions agent based on g TiO₂
3. Dispersant added and dissolved in water
4. Cowles turned on and TiO₂, added slowly to water-dispersant
5. To insure good dispersion of pigment; 45 minute mixing period followed by pigment addition.

B. Rheograms

1. Hercules Hi-Shear operating directions - Appendix I were followed.
2. Three Rheograms were run for each spring set: 25, 50, 100
3. Cup and bob, including coating, was held at constant 23°C throughout experiment by using a constant temperature water bath.
4. Rheograms were evaluated at the first Newtonian region break point (where W slope occurs).

FIGURE 5: RHEOGRAM SHOWING THE BREAK POINT AND
FIRST AND SECOND NEWTONIAN REGIONS

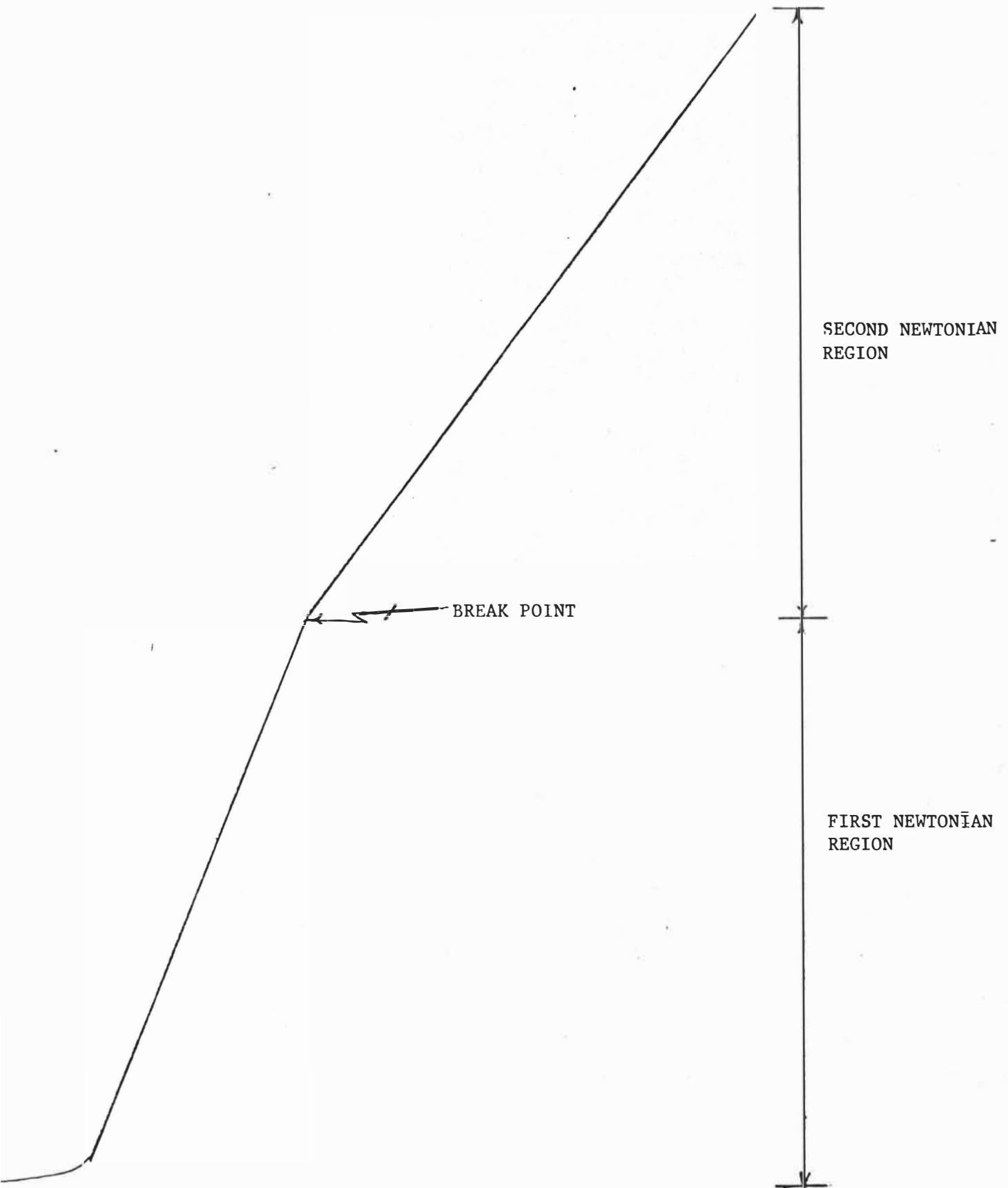


FIGURE 6
DISPERSANT LEVEL VS X_{EFF}

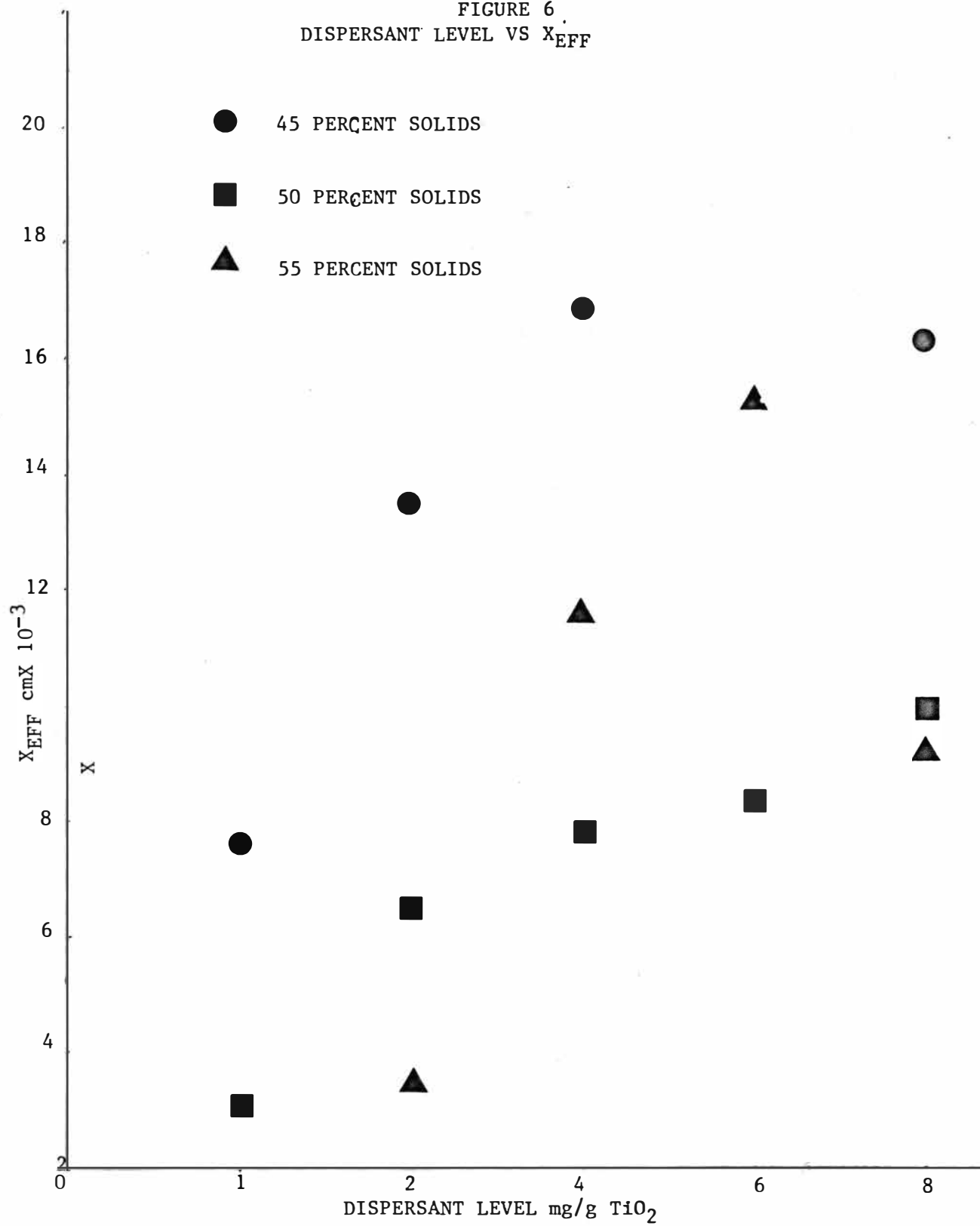


FIGURE 7
DISPERSANT LEVEL VS VISCOSITY

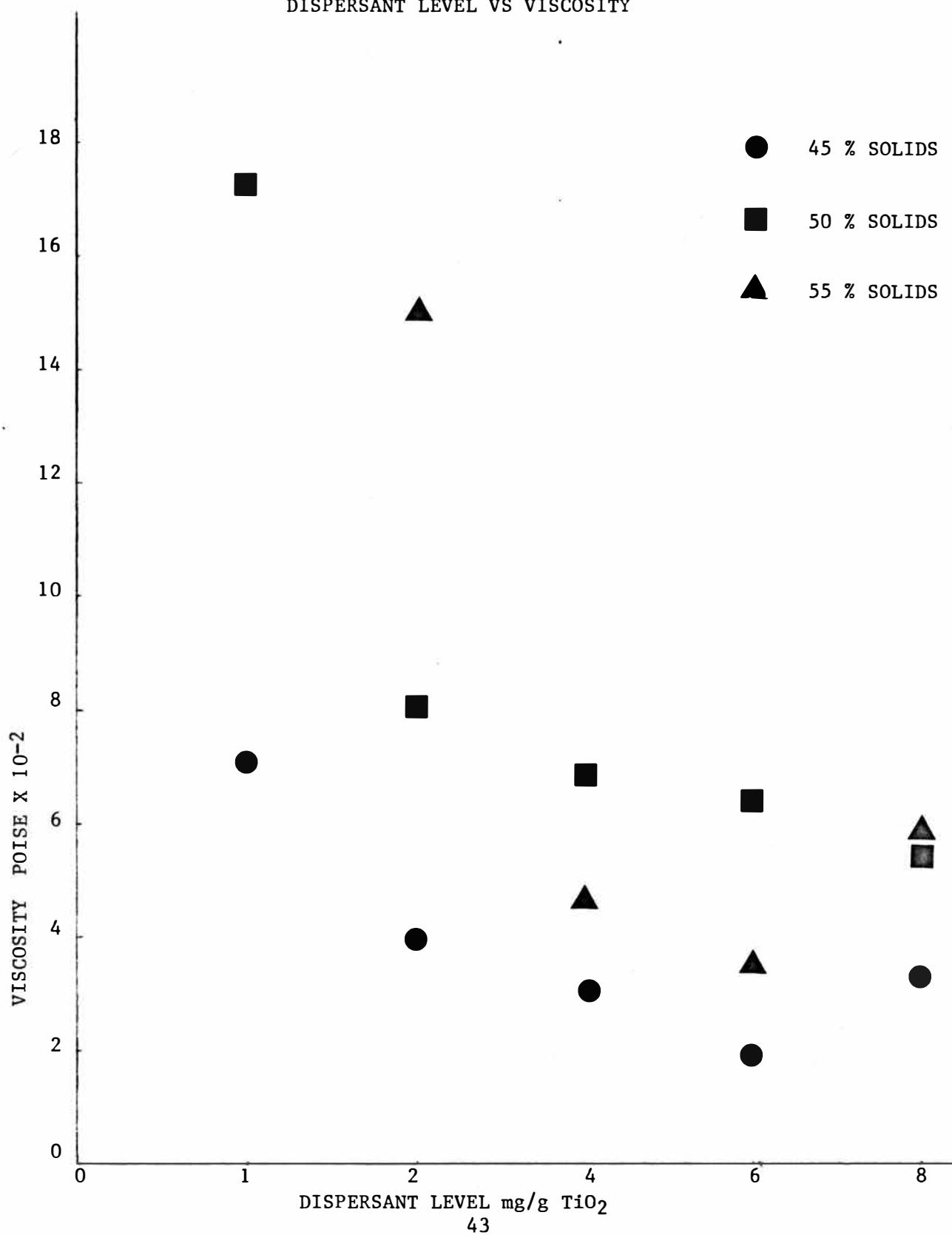
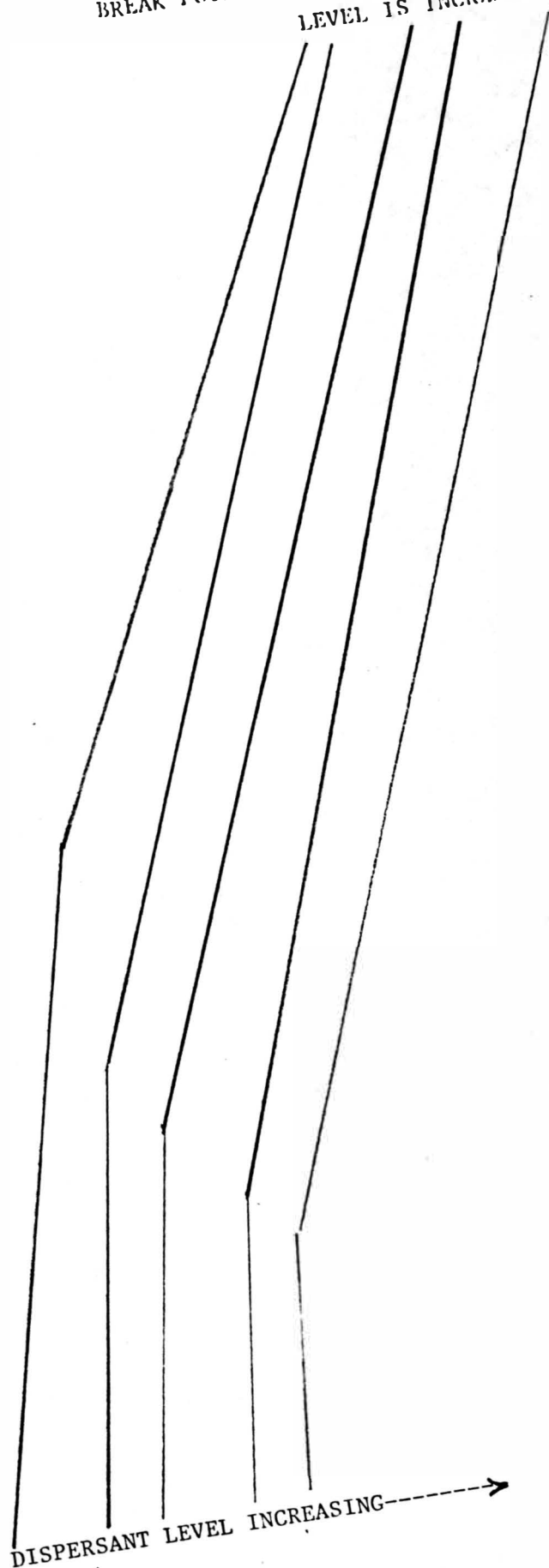


FIGURE 8
BREAK POINTS SEEN TO DECREASE IN RPM AS DISPERSANT
LEVEL IS INCREASED



50% SOLIDS
50,000 DYNE CM/CM SPRING SET

FIGURE 9
DISPERSANT LEVEL VS %RED

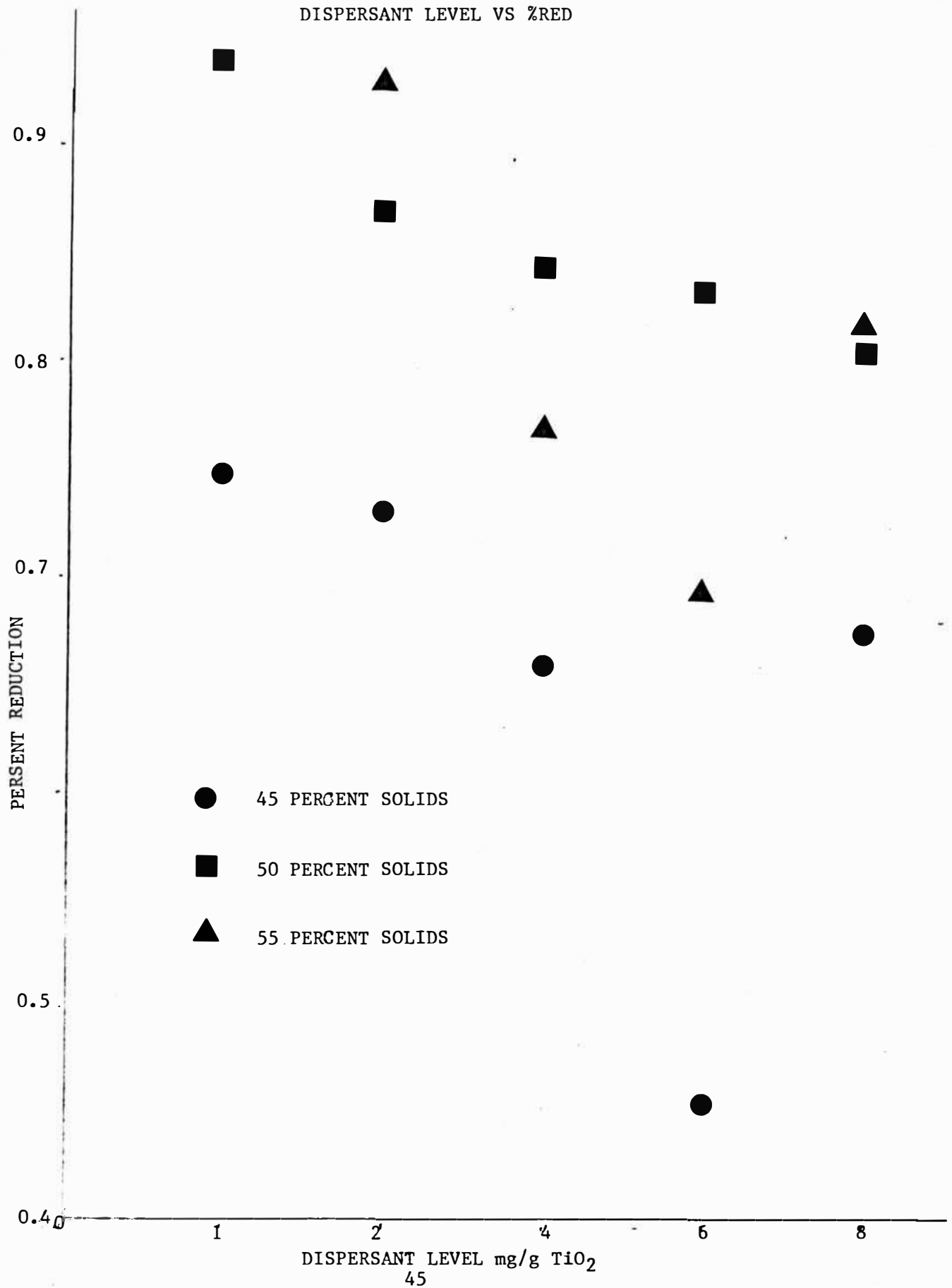
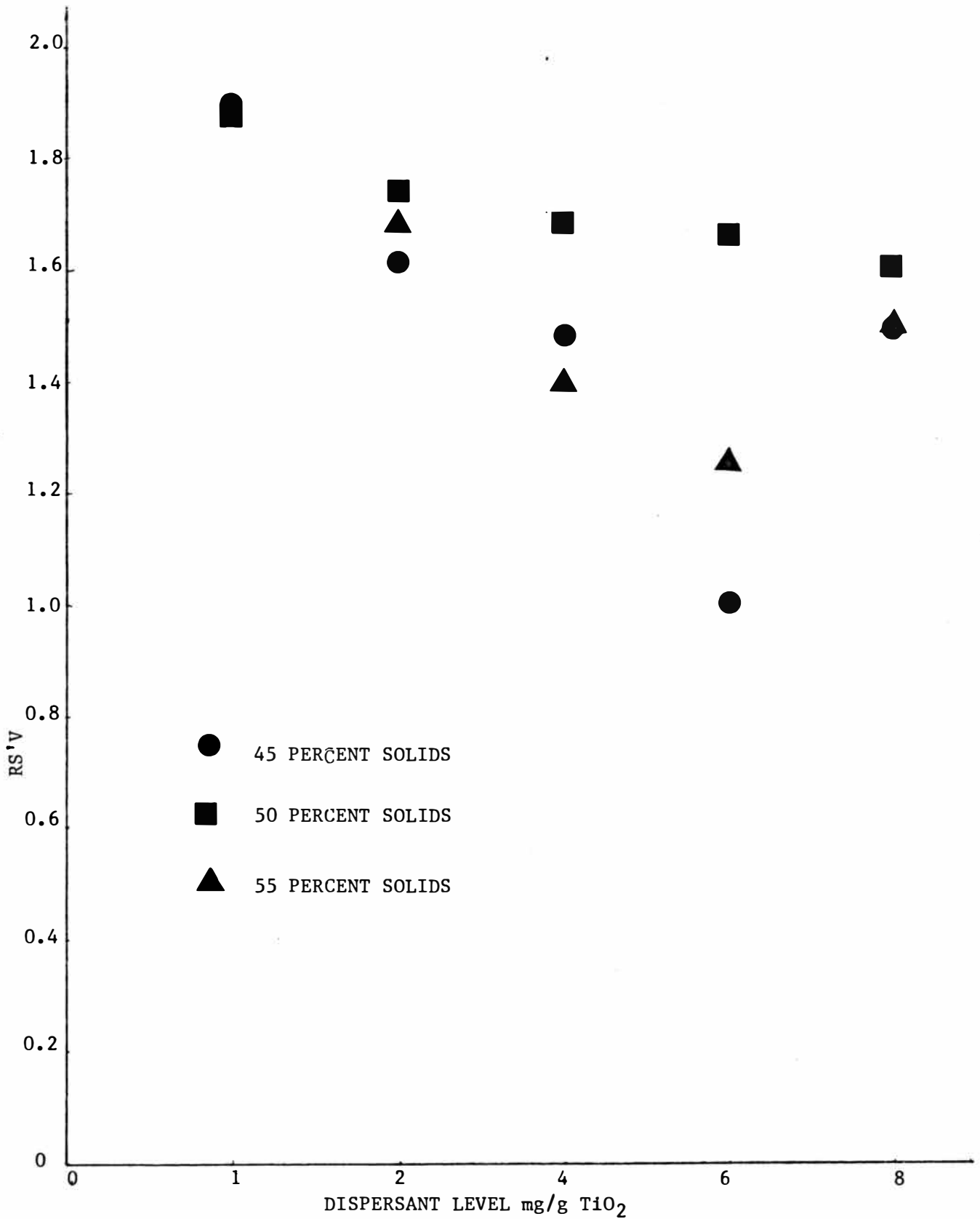


FIGURE 10
DISPERSANT LEVEL VS RS' V



APPENDIX 3

CODE	LEVEL	SPRING	DATA TABLES (RAW EXPERIMENTAL DATA)	TRQUE	RPM
------	-------	--------	-------------------------------------	-------	-----

DYNES.CM

X1A	1	25	54167	1210
X2A	1	50	46875	1284
X3A	1	100	40000	1191
X1B	2	25	19050	879
X2B	2	50	17463	854
X3B	2	100	12700	928
X1C	4	25	19050	773
X2C	4	50	12700	772
X3C	4	100	16933	842
X1D	6	25	7938	721
X2D	6	50	6350	624
X3D	6	100	21167	931
X1E	8	25	8996	635
X2E	8	50	15875	933
X3E	8	100	15875	810
X3E/5000	8	100	25400	1031
Y1A	1	25	166875	2152
Y2A	1	50	187500	2080
Y3A	1	100	185000	2178
Y1B	2	25	47083	1281
Y2B	2	50	59167	1396
Y3B	2	100	48333	1328
Y1C	4	25	30833	1032
Y2C	4	50	40833	1150
Y3C	4	100	36667	1143
Y1D	6	25	24000	930
Y2D	6	50	30833	924

CODE	LEVEL	SPRING	TROUE	RFM
------	-------	--------	-------	-----

DYNES.CM

Y1D	6	25	24000	930
Y2D	6	50	30833	924
Y3D	6	100	35000	1109
Y1E	8	25	4833	400
Y2E	8	50	24167	861
Y3E	8	100	31667	1040
Z3A/5000	1	100	598333	4027
Z2B	2	50	156667	2013
Z2B/5000	2	50	168750	2080
Z3B	2	100	156667	1898
Z3B/5000	2	100	185000	2235
Z1C	4	25	5417	554
Z2C/5000	4	50	16250	759
Z2C	4	50	17333	725
Z3C/5000	4	100	13333	684
Z1D	6	25	6667	395
Z2D/5000	6	50	8125	526
Z2D	6	50	9167	507
Z3D/5000	6	100	10000	743
Z3D	6	100	12500	566
Z1E	8	25	3750	335
Z2E/5000	8	50	8750	608
Z2E	8	50	15000	494
Z3E/5000	8	100	10000	697

VISC	WCR21	WCR22	WCR2	CTRPM	DRPM
------	-------	-------	------	-------	------

POISE				RPM	RPM
-------	--	--	--	-----	-----

.0855033	2.812951	1.644E-4	17114.33	1249.348	-39.3477
.0697284	1.870750	1.644E-4	11381.87	1018.850	265.1502
.0641478	1.583287	1.644E-4	9632.911	937.3076	253.6924
.0413942	.6592885	1.644E-4	4011.191	604.8393	274.1607
.0390566	.5869286	1.644E-4	3570.944	570.6830	283.3170
.0261390	.2628904	1.644E-4	1599.457	381.9352	546.0648
.0470705	.8524998	1.644E-4	5186.711	687.7798	85.22021
.0314210	.3798710	1.644E-4	2311.181	459.1138	312.8862
.0384110	.5676844	1.644E-4	3453.860	561.2492	280.7508
.0210285	.1701433	1.644E-4	1035.173	307.2626	413.7374
.0194367	.1453589	1.644E-4	884.3809	284.0031	339.9969
.0434253	.7255754	1.644E-4	4414.488	634.5174	296.4826
.0270588	.2817181	1.644E-4	1714.007	395.3754	239.6246
.0324987	.4063755	1.644E-4	2472.437	474.8605	458.1395
.0374336	.5391638	1.644E-4	3280.338	546.9689	263.0311
.0470553	.8519487	1.644E-4	5183.358	687.5574	343.4426
.1481093	8.440367	1.745E-4	48365.14	2100.243	51.75683
.1721755	11.40615	1.745E-4	65359.73	2441.510	-361.510
.1622360	10.12724	1.745E-4	58031.27	2300.565	-122.565
.0702018	1.896240	1.745E-4	10865.87	995.4869	285.5131
.0809520	2.521457	1.745E-4	14448.50	1147.928	248.0719
.0695151	1.859322	1.745E-4	10654.32	985.7488	342.2512
.0570650	1.252955	1.745E-4	7179.704	809.2015	222.7985
.0678183	1.769662	1.745E-4	10140.54	961.6876	188.3124
.0612721	1.444514	1.745E-4	8277.376	868.8598	274.1402
.0492903	.9348026	1.745E-4	5356.622	698.9544	231.0456

VISC	WCR21	WCR22	WCR2	CTRPM	DEPM
POISE				RPM	RPM
.0570650	1.252955	1.745E-4	7179.704	809.2015	222.7985
.0678183	1.769662	1.745E-4	10140.54	961.6876	188.3124
.0612721	1.444514	1.745E-4	8277.376	868.8598	274.1402
.0492903	.9348026	1.745E-4	5356.622	698.9544	231.0456
.0637347	1.562971	1.745E-4	8956.164	903.7834	20.21656
.0602795	1.398094	1.745E-4	8011.381	854.7853	254.2147
.0230776	.2049165	1.745E-4	1174.216	327.2483	72.75172
.0536109	1.105866	1.745E-4	6336.852	760.2215	100.7785
.0581577	1.301399	1.745E-4	7457.299	824.6965	215.3035
.2837884	30.98746	1.860E-4	166634.6	3898.396	128.6036
1486508	8.502190	1.860E-4	45720.41	2042.013	-29.0126
.1549579	9.238984	1.860E-4	49682.51	2128.654	-48.6542
.1576575	9.563700	1.860E-4	51428.66	2165.738	-267.738
.1580984	9.617268	1.860E-4	51716.72	2171.795	63.20477
.0186759	.1342028	1.860E-4	721.6735	256.5510	297.4490
.0408926	.6434081	1.860E-4	3459.918	561.7412	197.2588
.0456635	.8022963	1.860E-4	4314.337	627.2785	97.72150
.0372310	.5333433	1.860E-4	2868.046	511.4421	172.5579
.0322379	.3998803	1.860E-4	2150.351	442.8514	-47.8514
.0295033	.3349181	1.860E-4	1801.017	405.2867	120.7133
.0345345	.4588829	1.860E-4	2467.636	474.3992	32.60080
.0257066	.2542645	1.860E-4	1367.304	353.1310	389.8690
.0421820	.6846214	1.860E-4	3681.542	579.4531	-13.4531
.0213806	.1758380	1.860E-4	945.8353	293.7049	41.29514
.0274877	.2907182	1.860E-4	1563.333	377.5975	230.4025
.0579960	1.294172	1.860E-4	6959.391	796.6893	-302.689

CONC	NO	DENS	PF	VISC	XEFF	REDZ	RS'V
	FOISE	GMS/CM3		POISE	CM	%	
.45	.01056	1.522	.0568	.0855033	.0061752	.8764960	1.947769
.45	.01056	1.522	.0568	.0697284	.0075722	.8485552	1.885678
.45	.01056	1.522	.0568	.0641478	.0082310	.8353801	1.856400
.45	.01056	1.522	.0568	.0413942	.0127554	.7448918	1.655315
.45	.01056	1.522	.0568	.0390566	.0135188	.7296231	1.621385
.45	.01056	1.522	.0568	.0261390	.0201997	.5960061	1.324458
.45	.01056	1.522	.0568	.0470705	.0112172	.7756557	1.723679
.45	.01056	1.522	.0568	.0314210	.0168041	.6639189	1.475375
.45	.01056	1.522	.0568	.0384110	.0137461	.7250785	1.611286
.45	.01056	1.522	.0568	.0210285	.0251087	.4978254	1.106279
.45	.01056	1.522	.0568	.0194367	.0271651	.4566979	1.014884
.45	.01056	1.522	.0568	.0434253	.0121588	.7568239	1.681831
.45	.01056	1.522	.0568	.0270588	.0195130	.6097393	1.354976
.45	.01056	1.522	.0568	.0324987	.0162468	.6750635	1.500141
.45	.01056	1.522	.0568	.0374336	.0141050	.7179008	1.595335
.45	.01056	1.522	.0568	.0470553	.0112208	.7755831	1.723518
.5	.01056	1.616	.0568	.1481093	.0035649	.9287013	1.857403
.5	.01056	1.616	.0568	.1721755	.0030666	.9386672	1.877334
.5	.01056	1.616	.0568	.1622360	.0032545	.9349096	1.869819
.5	.01056	1.616	.0568	.0702018	.0075212	.8495765	1.699153
.5	.01056	1.616	.0568	.0809520	.0065224	.8695523	1.739105
.5	.01056	1.616	.0568	.0695151	.0075955	.8480905	1.696181
.5	.01056	1.616	.0568	.0570650	.0092526	.8149477	1.629895
.5	.01056	1.616	.0568	.0678183	.0077855	.8442898	1.688580
.5	.01056	1.616	.0568	.0612721	.0086173	.8276539	1.655308
.5	.01056	1.616	.0568	.0482807	.0107120	.7057582	1.571518

CONC	NO	DENS	PF	VISC	XEFF	HDZ	PSV
	POISE	GMS/CM3		POISE	CM	%	
.5	.01056	1.616	.0568	.0678183	.0077855	.8442898	1.688580
.5	.01056	1.616	.0568	.0612721	.0086173	.8276539	1.655308
.5	.01056	1.616	.0568	.0492903	.0107120	.7857592	1.571518
.5	.01056	1.616	.0568	.0637349	.0082843	.8343136	1.668627
.5	.01056	1.616	.0568	.0602795	.0087592	.8248162	1.649632
.5	.01056	1.616	.0568	.0230776	.0228794	.5424129	1.084826
.5	.01056	1.616	.0568	.0536109	.0098487	.8030251	1.606050
.5	.01056	1.616	.0568	.0581577	.0090788	.8184246	1.636849
.55	.01056	1.722	.0568	.2837884	.0018605	.9627892	1.750526
.55	.01056	1.722	.0568	.1486508	.0035519	.9289610	1.689020
.55	.01056	1.722	.0568	.1549579	.0034074	.9318525	1.694277
.55	.01056	1.722	.0568	.1576575	.0033490	.9330194	1.696399
.55	.01056	1.722	.0568	.1580984	.0033397	.9332062	1.696738
.55	.01056	1.722	.0568	.0186759	.0282717	.4345666	.7901210
.55	.01056	1.722	.0568	.0408926	.0129119	.7417627	1.348659
.55	.01056	1.722	.0568	.0456635	.0115628	.7687430	1.397715
.55	.01056	1.722	.0568	.0372310	.0141817	.7163657	1.302483
.55	.01056	1.722	.0568	.0322379	.0163782	.6724352	1.222610
.55	.01056	1.722	.0568	.0295033	.0178963	.6420743	1.167408
.55	.01056	1.722	.0568	.0345345	.0152891	.6942184	1.262215
.55	.01056	1.722	.0568	.0257066	.0205395	.5892105	1.071292
.55	.01056	1.722	.0568	.0421820	.0125172	.7496561	1.363011
.55	.01056	1.722	.0568	.0213806	.0246953	.5060942	.9201713
.55	.01056	1.722	.0568	.0274877	.0192086	.6158277	1.119687
.55	.01056	1.722	.0568	.0579960	.0091041	.8179183	1.487124